Genomic Analysis of *Citrobacter Portucalensis* Sb-2 Identifies a Phage Predation Driven Metalloid Resistance

Yanshuang Yu
Fujian Agriculture and Forestry University
Zhenchen Xie
Fujian Agriculture and Forestry University
Jigang Yang
Fujian Agriculture and Forestry University
Jinxuan Liang
Fujian Agriculture and Forestry University
YuanPing Li
Fujian Agriculture and Forestry University
Yong Guan Zhu
Institute of Urban Environment Chinese Academy of Sciences
Qiue Yang
Fujian Agriculture and Forestry University
Hend Alwathnani
King Saud University
Renwei Feng
Fujian Agriculture and Forestry University
Christopher Rensing (rensing@iue.ac.cn)
Fujian Agriculture and Forestry University https://orcid.org/0000-0002-5012-7953
Martin Herzberg
Martin-Luther-Universität Halle-Wittenberg: Martin-Luther-Universitat Halle-Wittenberg

Research Article

Keywords: HGT, phage, Enterobacteria, arsenite, antimonite, Citrobacter

Posted Date: April 30th, 2021

DOI: https://doi.org/10.21203/rs.3.rs-470342/v1

Abstract

Bacterial adaptation to extreme environments is often mediated by horizontal gene transfer (HGT). At the same time, phage mediated HGT for conferring bacterial arsenite and antimonite resistance has not been documented before. In this study, a highly arsenite and antimonite resistant bacterium, *C. portucalensis* strain Sb-2, was isolated and subsequent genome analysis showed that putative arsenite and antimonite resistance determinants were flanked or embedded by prophages. We predict these phage-mediated resistances play a significant role in maintaining genetic diversity within the genus of *Citrobacter* and are responsible for endowing the corresponding resistances to *C. portucalensis* strain Sb-2.

Highlights

- A gram-negative bacterium Sb-2 displaying a high resistance to arsenite (MIC 18 mM) and antimonite (MIC 60 mM) was isolated from farm soil near an antimony mine.
- Two clusters containing putative arsenite and antimonite resistance determinants flanked by or embedded in prophages were identified in Sb-2
- Phages in strain Sb-2 were suggested to be responsible for horizontal gene transfer of arsenite and antimonite resistance determinants and subsequent adaption to an extreme environment.
- YraQ (ArsP) is suggested to be a roxarsone (RoxIII) and MMA(III) efflux pump in Sb-2.

1 Introduction

Horizontal gene transfer (HGT) plays a pivotal role in adaptation of bacteria to extreme environments (Magaziner et al. 2019). There are three main mechanisms of HGT: bacterial conjugation, natural transformation and transduction (Sun 2018). Plasmids, transposons and genomic islands play a role in microbial adaptation to heavy metal contaminated environments (Ben Fekih et al. 2018; Dziewit et al. 2015; Hoostal et al. 2008). Phage predation has been proposed to play a significant role in maintaining genetic diversity within population of a single species. This is described by the operation of constant diversity dynamics, in which the diversity of prokaryotic populations is maintained by phage predation (Rodriguez-Valera et al. 2009). However, there is little direct evidence of phage-mediated transfer of heavy metal or metalloid resistance determinants. Essential metals such as Zn, Cu, Co and Ni play roles in metabolic processes as cofactors for enzymes or structural proteins or in signal transduction (Chandrangsu et al. 2017; Maret 2013; Tottey et al. 2007; Waldron and Robinson 2009). However, these metals have unique physico-chemical properties which are toxic in high amounts (Nies 1999; Tchounwou et al. 2012). Other metal(loids)s (e.g., As, Sb, Ag, Al, Au, Cd, Hg, and Pb) have no or limited biological roles and are only cytotoxic (Bruins et al. 2000). Regions of toxic metal(loid) pollutants are widespread around the world (Romaniuk et al. 2018). This is a consequence of both natural processes (e.g. weathering of metal-containing minerals, volcanic emissions, forest fires, deep sea springs and geysers) and anthropogenic activities (e.g. agriculture, animal husbandry, large-scale burning of fossil fuels, fracking, mining and metallurgical production (Charlesworth et al. 2011; Mason 2013; Nies 2008; Pujari and Kapoor 2021; Tchounwou et al. 2012; Williams and Silva 2006). The occurrence of heavy metals at high concentrations may significantly influence the taxonomic and functional diversities of soil microbial communities (Hoostal et al. 2008; Kandeler et al. 2000). Many microorganisms have developed efficient resistance mechanisms to toxic metal(loid)s. Three main mechanisms have been described; efflux of toxic ions from bacterial cells, enzymatic conversions of metal(loid)s and incorporation into complexes by metal-binding proteins such as metallothioneins and metallochaperones or small molecular compounds such as glutathione as metal buffers or sequestering processes (Blindauer 2015; Chandrangsu et al. 2017; Colvin et al. 2010; Isani and Carpene 2014; Martinez-Finley et al. 2012; Mazhar et al. 2020; Nies 2016; Silver and Phung le 2005).

Arsenic (As) and antimony (Sb) are toxic metalloids that often coexist in the environment (Lu et al. 2018; Shtangeeva et al. 2011) and share chemical and toxicological properties (Nies 1999). The toxicity of As and Sb depends upon their chemical species and oxidation state. In many bacterial species Sb(III) and As(III) are taken up by aquaglyceroporins such as the glycerol facilitator GlpF of *Escherichia coli*, producing toxicity (Meng et al. 2004; Sanders et al. 1997). Detoxification is frequently conferred by efflux via As(III)/Sb(III) efflux permeases such as ArsB and ACR3 permeases (Meng et al. 2004). Pentavalent inorganic arsenate (As(V)) enters cells of *E. coli* by phosphate uptake systems such as Pit and/or Pst. As(V) is reduced by ArsC arsenate reductases to the trivalent arsenite (As(III)), which is removed from the cells by the efflux permeases. Alternatively, As(III) is methylated by the ArsM As(III) S-adenosylmethionine methyltransferase, producing highly toxic methylarsenite (MAs(III)) and dimethylarsenite (DMAs(III)), as well as volatile trimethylarsenite (TMAs(III)). These are oxidized in air to the relatively nontoxic pentavalent species (Yang and Rosen 2016).

Sb(III) is also detoxified by efflux via ArsB or methylated by ArsM, but, in general, the comparable reactions with antimony are not well characterized (Butcher et al. 2000; Silver et al. 1981). Here we report isolation, of a highly antimony-resistant bacterium, *Citrobacter portucalensis* Sb-2, from an agricultural field near the biggest antimony mine in the world. From the draft sequence of its genome, we identified putative arsenic/antimony resistance genes and characterized its resistance to antimony and arsenic.

2 Materials And Methods

2.1 Culture enrichment and strain isolation

For bacterial enrichment, 1.0 g sample was mixed thoroughly with 20 mL of 0.85% saline, 50 ul suspension was inoculated into 5 mL minimal (Mergeay et al. 1985) / R2A (Zhang et al. 2020) and TY media (Mergeay et al. 1985) respectively containing 0.5 mM potassium antimonyl tartrate ($C_8H_4K_2O_{12}Sb_2{\cdot}3H_2O$) or sodium arsenite ($NaAsO_2$). The cultures were incubated at 28°C with 180 rpm shaking for about 1 day until the medium became turbid. The culture was transferred to fresh medium containing twice the concentrations of Sb(III) or As(III). The concentrations of Sb(III) or As(III) were gradually increased until the cultures stopped growing. The microbial suspension was subsequently serially diluted onto agar plates with 4 mM Sb(III) or As(III). Single colonies were

picked and re-streaked at least three times to obtain pure isolates. Metal(loid) concentrations from the isolation site were determined by inductively coupled plasma mass spectroscopy (ICP-MS) (NexIon 300 X, PerkinElmer, US).

2.2 Phylogenetic analysis and genome sequencing

Total genomic DNA of *Citrobacter portucalensis* Sb-2 was extracted using a TIANamp Bacteria DNA kit (TIANGEN, China) following the suggestions of manufacturer and used as a template to amplify 16S rRNA sequence by PCR. Close relative and phylogenetic affiliation of the obtained 16S rRNA sequences were determined by using the BLAST search program at the NCBI website (www.ncbi.nlm.nih.gov). The 16S rRNA gene sequences were submitted for comparison and identification to the GenBank databases using the NCBI Blastn algorithm and to the EMBL databases using the Fasta algorithm. The phylogenetic tree of 16S rRNA gene sequences and the amino acid sequences of compared resistance determinants were inferred by Geneious prime 2021.1.1. (Geneious Tree Builder) (https://www.geneious.com), global alignment, gap open penalty 12, gap extension penalty 3, Blosum62 cost matrix, Jukes-Cantor, Neighbor-Joining, Resampling Method - Bootstrap; with 100 replicates. Genome sequencing was performed on the Illumin Hiseq X ten System sequencing platform (Illumina, CA, USA). The sequencing library was constructed with an Illumina Nextera XT library prep kit (Illumina, San Diego, CA, USA). Morphological and physiological experiments were done to further characterize the bacterium (Kearse et al. 2012).

2.3 Determination of the Minimal Inhibitory Concentration (MIC)

The single colonies were later used to examine the minimal inhibitory concentration (MIC) on $C_8H_4K_2O_{12}Sb_2{\cdot}3H_2O$, $NaAsO_2$, $CuSO_4{\cdot}5H_2O$ and $ZnSO_4{\cdot}7H_2O$, supplemented mineral salts media (gluconate 2 g L^{-1} as sole carbon source) cultures plates. Mineral salts medium contained (1000 ml of ddH_2O) Tris 6.06 g pH 7.0, NaCl 4.68 g, KCl 1.49 g, NH_4Cl 1.07 g, Na_2SO_4 0.43 g, $MgCl_2{\cdot}6H_2O$ 0.20 g, $CaCl_2{\cdot}2H_2O$ 0.03 g, $Na_2HPO_4{\cdot}12H_2O$ 0.23 g, Fe(III)NH_4 citrate 0.005 g, sodium gluconate 2 g, 1 ml of the trace element solution SL 7 and Difco Bacto Agar 15 g L^{-1} (Nies et al. 2006). Mineral salts medium is a Tris-buffered and low phosphate medium designed to reduce metal complexation and determine accurate MICs (Mergeay et al. 1985).

2.4 Scanning electron microscopy

Overnight cultures were diluted 1:100 in fresh mineral salts medium and incubated at 28°C. Samples were harvested at a logarithmic phase by centrifuging for 5 min, 2500 rpm at 4°C and were immobilized using glutaraldehyde (5%, v/v) for 4 h. Samples were washed three times in 0.1M phosphate buffer solution (PBS) at 10–15 min intervals prior to a 4 h treatment with secondary fixative in osmium acid (1%, v/v). After three washes with ddH_2O at 10–15 min intervals, samples were chemically dehydrated in a graded of ethanol-water solutions (ethanol 50%, 70%, 80%, 90% and 100% [3×]), v/v) at 10–15 min intervals. The samples were then attached to SEM specimen mounts for light drying and sputter-coated with gold prior to observation under SEM (JSM-6380LV, JEOL, Japan)

2.5 Genome annotation and characterization

The shot gun sequence of *Citrobacter portucalensis* Sb-2 was submitted to NCBI Prokaryotic Genome Annotation Pipeline (PGAP; Annotation Software revision 4.6) for gene annotation following the standard operating procedures and was released on 26rd of December, 2020 with GenBank assembly accession number GCA_016406035.1, under BioProject: PRJNA684029 and BioSample: SAMN017050479.

3 Results And Discussion

3.1 Enrichment of the most antimonite and arsenite resistant bacteria

The metal(loid) concentrations of isolation site were shown in Table 1, other physicochemical parameters of soil were as follows: pH: 7.95; total phosphorus 0.2663 g kg^{-1}; total nitrogen 0.0221 mg kg^{-1}; available phosphorus 16.6175 mg kg^{-1}; available potassium 85.00 mg kg^{-1}; organic matter 40.6704 g kg^{-1}; electrical conductivity 98.60 uS cm^{-1}. For bacterial isolation, enrichment cultures of a heavy metal contaminated chili peppers field (high concentration of contamination: 670 mg kg^{-1} Sb & 138 mg kg^{-1} As) near the biggest antimony mine in the world were performed to obtain the most antimonite and arsenite resistant microbes. For the isolates from this site, genus of *Microbacterium* and *Pseudochrobactrum* were obtained when performing As enrichment, while genus of *Citrobacter*, *Pseudomonas* and *Enterobacter* were obtained from Sb enrichment. Among them, *C. portucalensis* strain Sb-2 was one of the most antimonite resistant isolates and was further characterized here. The general features of Sb-2 are shown in Table 2.

C. portucalensis strain Sb-2 was highly resistant to arsenite (MIC 18 mM) and extremely resistant to antimonite (MIC 60 mM), with MICs much higher than the well-studied metal resistant bacteria *Cupriavidus metallidurans* AE104 & CH34 (MIC 2.5 mM for arsenite; 0.6 mM for antimonite) and well-studied strain *Escherichia coli* W3110 (MIC 3 mM for arsenite; 0.8 mM for antimonite) on the same solid minimal medium (Table 3).

3.2 Morphology, Growth and Physiology of Sb-2

The isolated strain *C. portucalensis* strain Sb-2 was shown to be a gram negative, motile Gammaproteobacterium with a morphology of short rods and forms creamy white colonies on minimal medium (Figure 1). 16S sequencing was performed to determine phylogeny and it could be determined to be most closely related to *Citrobacter portucalensis* (Figure 2). The genus *Citrobacter* belongs to the family of Enterobacteriaceae and is sorted in the “CESP” or “ESCPM” (Citrobacter, Enterobacter, Serratia and Providencia, and more recently, Morganella and Hafnia genres) group.

3.3 Genome and the phage driven arsenic and antimony resistance determinants of strain Sb-2

For the purpose of understanding the genetic mechanism for As(III) and Sb(III) resistance to *Citrobacter portucalensis* Sb-2, the whole genome of strain Sb-2 was sequenced and gene functions was annotated, the project of Sb-2 was shown in Table 4. The genome size of *C. portucalensis* Sb-2 is 4,794,853 bp, with a 51.9 mol% GC content, consists of 37 DNA Scaffolds (Table 5). The chromosome contains 4,625 Coding Sequences (CDS), 8 rRNAs, and 73 tRNAs (Table 5).

To better understand the genomic basis underlying this metalloid resistant phenotype, the draft genome sequence of *C. portucalensis* Sb-2 was analyzed using bioinformatics techniques for occurrence, homology and synteny in the genus *Citrobacter*. Furthermore, the clusters found were compared with the chromosomally encoded and well-studied reference determinant of the *E. coli* wild-type strain K12 to highlight similarities and uniqueness at the sequence level and synteny (Diorio et al. 1995; Oden et al. 1994; Silver et al. 1981). Two resistance gene clusters could be identified on the genome of strain Sb-2 (Figure 3). Both are higher in complexity of construction compared to the chromosomal encoded of *E. coli* K12. The operon encoding the arsenic resistance mediating components in *E. coli* K12 contains the *arsR*, *arsB* and *arsC* genes encoding the transcriptional repressor (ArsR), the transmembrane efflux protein (ArsB) and the arsenic reductase (ArsC) (Busenlehner et al. 2003; Meng et al. 2004; Zhu et al. 2014). A more complex operon structure occurs in *E. coli* R773 with two additional genes, *arsD* and *arsA* (Chen et al. 1986). Here, in addition to the efflux only mediated by ArsB, arsenite transporter exist that are composed of an ArsB pore plus an ArsA ATPase (Castillo and Saier 2010; Dey and Rosen 1995; Yang et al. 2012). The gene *arsD* encoding an arsenic metallochaperone that transfers trivalent metalloids to the ArsAB pump with an additional function as an inducer-independent, weak repressor of the *ars* operon. The ars_1-cluster (locus tag: I9P40_RS1120 - I9P40_RS1120), one of the identified *ars* clusters, in strain Sb-2 contains all these five components, but also a second *arsR* gene ($arsR_1$, I9P40_RS1120) and a gene encoding an uncharacterized gene product YraQ (*yraQ*, I9P40_RS1125) in a divergon orientation (Figure 3). This gene product is generally annotated as a permease and predicted to be transporter with eight transmembrane helices (Aziz et al. 2008; Kelley et al. 2015; Krogh et al. 2001). YraQ from Sb-2 is no ortholog to the *yraQ* (locus tag: b13151) encoded gene product of *E. coli* K12 and shares only 18.5 % of amino acid (AA) identity with different topology (data not shown). Furthermore, this gene is encoded independently of an arsenic cluster on the chromosome of *E. coli*. In contrast, YraQ from Sb-2 displayed significant homologies to ArsP (~ 90% identity on AA level) from *Campylobacter jejunii* and is therefore predicted to confer resistance to roxarsone and MMA(III) (Shen et al. 2014), suggesting YraQ could also have a high efficiency in conferring roxarsone and MMA(III) resistance to Sb-2. The second ars_2-cluster (locus tag: I9P40_RS10540 - I9P40_RS10555) of strain Sb-2 is homologous in synteny with simple cluster of *E. coli* K12 but with the additional gene *arsH* (I9P40_RS10540) in a divergon orientation to *arsR* (I9P40_RS10545). The encoded gene products show a higher degree of AA identity to the *E. coliars* operon when compared to the gene products of ars_1-cluster (Figure 3). Both clusters are found independently and frequently on the genomes of other *C. portucalensis* strains and *Citrobacter* species. Sometimes only the simple cluster 2 is present, as in *C. braakii* FDAARGOS_253, or only the more complex cluster 1 in *C. portucalensis* P10159 and *C. freundii* RHB12-C20. In the genome of *C. freundii* R17, an intact cluster and a $cluster_1$ with an interrupted *arsD´* can be identified (Figure 3).

Interestingly, both arsenic resistance determinants of strain Sb-2 are flanked by DNA region belonging to prophage Klebsi_phiKO2 (NC_005857) (ars_2 - cluster) or embedded in prophage Entero_mEp237 (N C_019704) DNA region (ars_1 - cluster) respectively (Table 6). Both phages flanking *arsH* <-> *arsRBC* clusters in the genomes of *C. braaki* strain FDAARGOS_253 and *C. portucalensis* Sb-2 strains show the same closest relative, PHAGE_Klebsi_phiKO2, according to PHASTER annotation (Arndt et al. 2019). In comparison, the more complex *arsRDABC* <-> $arsR_1$ <-> *yraQ* clusters in *C. portucalensis* strain Sb-2 and P10159 as well as in *C. freundii* RHB12-C20 are embedded in the homologous annotated phage, Entero_mEp237. This arrangement displays a corresponding degree of similarity within these two *ars* clusters and the respective flanking and enclosing prophages in the genomes of these members of the *Citrobacter* genus. This finding gives a direct indication for phage-driven HGT metalloid resistance spread. These phages are widespread in the *Enterobacteriacea* family and, due to their broad host range, enable not only horizontal gene spread and transmission of metal resistance determinants, but also of antibiotic resistance islands or virulence factors (Ekundayo and Okoh 2018; Magaziner et al. 2019). The results of comparative phageomics of the five *Citrobacter* species shown in Table 6 indicate that strain Sb-2 harbors, in addition to two mentioned intact phages (size of 59.3 and 25.5 kb), another intact phage of size 34.4 kb, an incomplete and a questionable phage, most similar to PHAGE_Salmon_SP_004 (NC_021774;), PHAGE_Pectob_CBB (NC_041878) and PHAGE_Escher_500465_1 (NC049342). Comparable in number of harbored prophages is *C. braaki* strain 253 with 4 intact and one incomplete and *C. freudii* strain R17 with two intact, two incomplete and two questionable. In contrast, the genome of *C. portucalensis* P10159 followed by *C. freudii* RHB12-20 displayed a higher number of phage DNA regions with up to 5 intact, 4-10 incomplete and also up to five questionable.

The presence of these putative arsenite and antimonite resistance determinants flanked and embedded by prophages and present in different *Citrobacter* species from different environments indicates widespread transduction of this phage. It is possible that this determinant also protects *Citrobacter* species from protist predation that are known to use both arsenite in addition to copper and zinc to poison the prey (Hao et al. 2017).

4 Conclusion

The contamination of heavy metals at high concentrations in different areas around the world is predicted to significantly influence the taxonomic and functional diversities of soil microbial communities. Here we showed evidence that phage predation plays a major role in maintaining genetic diversity within population of a single species or genus. These results support a better understanding of diversity dynamics, in which the diversity of prokaryotic populations is driven by phage predation. In addition, the role of HGT in adaptation of bacteria to extreme environments is highlighted.

Declarations

Data availability

This Whole Genome Shotgun project has been deposited at DDBJ/ENA/GenBank under the accession JAEKIJ000000000. The data used to support the findings of this study are included within the article. Please check https://www.ncbi.nlm.nih.gov/assembly/ GCF_016406035.1 for more details.

Declaration of competing interest

The authors declare that they have no known competing financial interests or personal relationships that could have appeared to influence the work reported in this paper.

Acknowledgements

This work was supported by NSFC grant number (31770123) and the Natural Science Foundation of Fujian province (2018J01668). We also acknowledge Researchers Supporting Project number (RSP-2020/205), King Saud University, Riyadh, Saudi Arabia.

References

1. Arndt D, Marcu A, Liang Y, Wishart DS (2019) PHAST, PHASTER and PHASTEST: Tools for finding prophage in bacterial genomes. Brief Bioinform 20(4):1560–1567
2. Aziz RK, Bartels D, Best AA, DeJongh M, Disz T, Edwards RA, Formsma K, Gerdes S, Glass EM, Kubal M, Meyer F, Olsen GJ, Olson R, Osterman AL, Overbeek RA, McNeil LK, Paarmann D, Paczian T, Parrello B, Pusch GD, Reich C, Stevens R, Vassieva O, Vonstein V, Wilke A, Zagnitko O (2008) The RAST server: Rapid annotations using subsystems technology. BMC Genom 9(1):1–15
3. Ben Fekih I, Zhang C, Li YP, Zhao Y, Alwathnani HA, Saquib Q, Rensing C, Cervantes C (2018) Distribution of arsenic resistance genes in prokaryotes. Front Microbiol 9:2473
4. Blindauer CA (2015) Advances in the molecular understanding of biological zinc transport. Chem Commun 51(22):4544–4563
5. Bruins MR, Kapil S, Oehme FW (2000) Microbial resistance to metals in the environment. Ecotoxicol Environ Saf 45(3):198–207
6. Busenlehner LS, Pennella MA, Giedroc DP (2003) The SmtB/ArsR family of metalloregulatory transcriptional repressors: structural insights into prokaryotic metal resistance. FEMS Microbiol Rev 27(2–3):131–143
7. Butcher BG, Deane SM, Rawlings DE (2000) The chromosomal arsenic resistance genes of Thiobacillus ferrooxidans have an unusual arrangement and confer increased arsenic and antimony resistance to Escherichia coli. Appl Environ Microb 66(5):1826–1833
8. Castillo R, Saier MH (2010) Functional promiscuity of homologues of the bacterial ArsA ATPases. Int J Microbiol 2010:187373
9. Chandrangsu P, Rensing C, Helmann JD (2017) Metal homeostasis and resistance in bacteria. Nat Rev Microbiol 15(6):338–350
10. Charlesworth S, De Miguel E, Ordonez A (2011) A review of the distribution of particulate trace elements in urban terrestrial environments and its application to considerations of risk. Environ Geochem Hlth 33(2):103–123
11. Chen CM, Misra TK, Silver S, Rosen BP (1986) Nucleotide sequence of the structural genes for an anion pump. The plasmid-encoded arsenical resistance operon. J Biol Chem 261(32):15030–15038
12. Colvin RA, Holmes WR, Fontaine CP, Maret W (2010) Cytosolic zinc buffering and muffling: their role in intracellular zinc homeostasis. Metallomics 2(5):306–317
13. Dey S, Rosen BP (1995) Dual mode of energy coupling by the oxyanion-translocating ArsB protein. J Bacteriol 177(2):385–389
14. Diorio C, Cai J, Marmor J, Shinder R, Dubow MS (1995) An Escherichia-coli chromosomal ars operon homolog is functional in arsenic detoxification and is conserved in gram-negative bacteria. J Bacteriol 177(8):2050–2056
15. Dziewit L, Pyzik A, Szuplewska M, Matlakowska R, Mielnicki S, Wibberg D, Schlüter A, Pühler A, Bartosik D (2015) Diversity and role of plasmids in adaptation of bacteria inhabiting the Lubin copper mine in Poland, an environment rich in heavy metals. Front Microbiol 6:152
16. Ekundayo TC, Okoh AI (2018) Pathogenomics of virulence traits of Plesiomonas shigelloides that were deemed inconclusive by traditional experimental approaches. Front Microbiol 9:3077
17. Hao X, Li X, Pal C, Hobman J, Larsson DGJ, Saquib Q, Alwathnani HA, Rosen BP, Zhu YG, Rensing C (2017) Bacterial resistance to arsenic protects against protist killing. Biometals 30(2):307–311
18. Hoostal MJ, Bidart-Bouzat MG, Bouzat JL (2008) Local adaptation of microbial communities to heavy metal stress in polluted sediments of Lake Erie. FEMS Microbiol Ecol 65(1):156–168
19. Isani G, Carpene E (2014) Metallothioneins, unconventional proteins from unconventional animals: a long journey from nematodes to mammals. Biomolecules 4(2):435–457
20. Kandeler E, Tscherko D, Bruce KD, Stemmer M, Hobbs PJ, Bardgett RD, Amelung W (2000) Structure and function of the soil microbial community in microhabitats of a heavy metal polluted soil. Biol Fert Soils 32(5):390–400
21. Kearse M, Moir R, Wilson A, Havas SS, Cheung M, Sturrock S, Buxton S, Cooper A, Markowitz S, Duran C, Thierer T, Ashton B, Meintjes P, Drummond A (2012) Geneious Basic: an integrated and extendable desktop software platform for the organization and analysis of sequence data. Bioinformatics 28(12):1647–1649
22. Kelley LA, Mezulis S, Yates CM, Wass MN, Sternberg MJE (2015) The Phyre2 web portal for protein modeling, prediction and analysis. Nat Protoc 10(6):845–858
23. Krogh A, Larsson B, von Heijne G, Sonnhammer EL (2001) Predicting transmembrane protein topology with a hidden Markov model: application to complete genomes. J Mol Biol 305(3):567–580
24. Lu X, Zhang Y, Liu C, Wu M, Wang H (2018) Characterization of the antimonite- and arsenite-oxidizing bacterium Bosea sp. AS-1 and its potential application in arsenic removal. J Hazard Mater 359:527–534
25. Magaziner SJ, Zeng ZY, Chen BH, Salmond GPC (2019) The prophages of citrobacter rodentium represent a conserved family of horizontally acquired mobile genetic elements associated with enteric evolution towards pathogenicity. J Bacteriol 201(9)
26. Maret W (2013) Zinc biochemistry: from a single zinc enzyme to a key element of life. Adv Nutr 4(1):82–91

27. Martinez-Finley EJ, Chakraborty S, Fretham SJ, Aschner M (2012) Cellular transport and homeostasis of essential and nonessential metals. Metallomics 4(7):593–605
28. Mason RP (2013) Trace metals in aquatic systems. Wiley-Blackwell, Chichester, pp 219–309
29. Mazhar SH, Herzberg M, Ben Fekih I, Zhang CK, Bello SK, Li YP, Su JM, Xu JQ, Feng RW, Zhou SG, Rensing C (2020) Comparative insights into the complete genome sequence of highly metal resistant cupriavidus *metallidurans* strain BS1 isolated from a gold-copper mine. Front Microbiol 11:47
30. Meng YL, Liu Z, Rosen BP (2004) As(III) and Sb(III) uptake by GlpF and efflux by ArsB in Escherichia coli. J Biol Chem 279(18):18334–18341
31. Mergeay M, Nies D, Schlegel HG, Gerits J, Charles P, Van Gijsegem F (1985) *Alcaligenes eutrophus* CH34 is a facultative chemolithotroph with plasmid-bound resistance to heavy metals. J Bacteriol 162(1):328–334
32. Nies DH (1999) Microbial heavy-metal resistance. Appl Microbiol Biotechnol 51(6):730–750
33. Nies DH (2008) Essential and toxic effects of elements on microorganisms elements and their compounds in the environment. Wiley-VCH Verlag GmbH, pp 256–276
34. Nies DH (2016) The biological chemistry of the transition metal "transportome" of Cupriavidus metallidurans. Metallomics 8(5):481–507
35. Oden KL, Gladysheva TB, Rosen BP (1994) Arsenate reduction mediated by the plasmid-encoded arsc protein is coupled to glutathione. Mol Microbiol 12(2):301–306
36. Pujari M, Kapoor D (2021) Heavy metals in the ecosystem: Sources and their effects. In: Heavy Metals in the Environment. Elsevier, pp 1–7
37. Rodriguez VF, Martin CAB, Rodriguez BB, Pasic L, Thingstad TF, Rohwer F, Mira A (2009) Explaining microbial population genomics through phage predation. Nat Rev Microbiol 7(11):828–836
38. Romaniuk K, Ciok A, Decewicz P, Uhrynowski W, Budzik K, Nieckarz M, Pawlowska J, Zdanowski MK, Bartosik D, Dziewit L (2018) Insight into heavy metal resistome of soil psychrotolerant bacteria originating from King George Island (Antarctica). Polar Biol 41(7):1319–1333
39. Sanders OI, Rensing C, Kuroda M, Mitra B, Rosen BP (1997) Antimonite is accumulated by the glycerol facilitator GlpF in Escherichia coli. J Bacteriol 179(10):3365–3367
40. Shen Z, Luangtongkum T, Qiang Z, Jeon B, Wang L, Zhang Q (2014) Identification of a novel membrane transporter mediating resistance to organic arsenic in Campylobacter jejuni. Antimicrob Agents Chemother 58(4):2021–2029
41. Shtangeeva I, Bali R, Harris A (2011) Bioavailability and toxicity of antimony. J Geochem Explor 110(1):40–45
42. Silver S, Budd K, Leahy KM et al (1981) Inducible plasmid-determined resistance to arsenate, arsenite, and antimony (III) in escherichia coli and Staphylococcus aureus. J Bacteriol 146(3):983–996
43. Silver S, Phung le T (2005) A bacterial view of the periodic table: genes and proteins for toxic inorganic ions. J Ind Microbiol Biotechnol 32(11–12):587–605
44. Sun D (2018) Pull in and push out: Mechanisms of horizontal gene transfer in bacteria. Front Microbiol 9:2154
45. Tchounwou PB, Yedjou CG, Patlolla AK, Sutton DJ (2012) Heavy metal toxicity and the environment. Exp Suppl 101:133–164
46. Tottey S, Harvie D, Robinson N (2007) Understanding how cells allocate metals. Molecular Microbiology of Heavy Metals, vol 6. Springer, Berlin Heidelberg, pp 3–35 Microbiology Monographs
47. Waldron KJ, Robinson NJ (2009) How do bacterial cells ensure that metalloproteins get the correct metal. Nat Rev Microbiol 7(1):25–35
48. Williams RJP, Silva JJRFd (2006) The chemistry of evolution: The development of our ecosystem. Elsevier, Amsterdam; Boston
49. Yang HC, Fu HL, Lin YF, Rosen BP (2012) Pathways of arsenic uptake and efflux. Metal Transporters 69:325–358
50. Yang HC, Rosen BP (2016) New mechanisms of bacterial arsenic resistance. Biomed J 39(1):5–13
51. Zhang J, Chai CW, Thomasarrigo LK, Zhao SC, Kretzschmar R, Zhao FJ (2020) Nitrite accumulation is required for microbial anaerobic iron oxidation, but not for arsenite oxidation, in two *Heterotrophic denitrifiers*. Environ Sci Technol 54(7):4036–4045
52. Zhou Y, Liang Y, Lynch KH, Dennis JJ, Wishart DS (2011) PHAST: a fast phage search tool. Nucleic Acids Res 39(Web Server issue):W347-52
53. Zhu YG, Yoshinaga M, Zhao FJ, Rosen BP (2014) Earth abides arsenic biotransformations. Annu Rev Earth Planet Sci 42:443–467

Tables

Table 1 - Metal (loid) concentrations of isolation site

Metals (metalloids)	**Sb**	**As**	Cr	Pb	Cd	Mn	Cu
Concentrations（mg kg^{-1}）	**670.281**	**137.992**	100.868	54.862	12.36	677.169	53.888

Table 2 - Classification and general features of Citrobacter portucalensis strain Sb-2

MIGS ID	Property	Term	Evidence code[a]
	classification	Domain *Bacteria*	TAS
		Phylum *Proteobacteria*	TAS
		Class *Gammaproteobacteria*	TAS
		Order *Enterobacteriales*	TAS
		Family *Enterobacteriaceae*	TAS
		Genus *Citrobacter*	TAS
		Species *Citrobacter portucalensis*	TAS
		Type strain: Sb-2	
	Gram stain	Negative	
	Cell shape	Rods	
	Motility	Motile	
	Sporulation	Nonspore-forming	
	Temperature range	Mesophile, 20 - 35°C	
	Optimum temperature	30°C	
	pH range	5 - 9	
MIG-6	Habitat	Soil and water	
MIG-6.3	Salinity	No growth with > 3.5% NaCl (w/v)	
MIG-22	Oxygen requirement	Aerobic	
MIG-15	Biotic relationship	Free-living	
MIG-14	Pathogenicity	Not reported	
MIG-4	Geographic location	Farm soil near antimony mine, Lengshuijiang, Hunan, China	
MIG-5	Sample collection	07/21/2019	
MIG-4.1	Latitude	N27° 11.027'	
MIG-4.2	Longitude	E111° 24.414'	
MIG-4	Altitude	509 m	

[a]Evidence codes - IDA Inferred from Direct Assay. TAS Traceable Author Statement (i.e.. a direct report exists in the literature). NAS Non-traceable Author Statement (i.e.. not directly observed for the living, isolated sample, but based on a generally accepted property for the species or anecdotal evidence).

These evidence codes are from the Gene Ontology project [55]

Table 3 - Minimal inhibitory concentration (MIC) of selected heavy metals (metalloids) for Citrobacter sp. Sb-2, Escherichia coli K12 - W3110 and Cupriavidus metallidurans AE104 & CH34 on solid mineral salts medium (mean values of 3 replicates are given in the table)

Metals (metalloids)	As^{3+} (mM)	Sb^{3+} (mM)	Cu^{2+} (mM)	Zn^{2+} (mM)
Sb-2	**18**	**60**	0.4	2-4
W3110	3	0.8	0.2	1
CH34	2.5	0.8	4.5	12
AE104	2.5	0.6	2.5	< 0.5

Table 4 - Project information

MIGS ID	Property	Term
MIG-31	Finishing quality	High-Quality Draft – Scaffold_x37
MIG-28	Libaries used	Illumina Paired-end library
MIG-29	Sequencing plateforms	Illumina HiSeq
MIG-31.2	Fold coverage	290.0x
MIG-30	Assemblers	SOAPdenovo v. 2.3
MIG-32	Gene calling method	NCBI Prokaryotic Genome Annotation Pipeline (PGAP)
	Locus taq	I9P40_
	Genbank ID	GCA_016406035.1
	GenBank Date of Realease	2020/12/26
	BioSample	SAMN17050479
	BioProject	PRJNA684029
	WGD Project	JAEKIJ01
	Project relevance	Environmental, heavy metal resistance

Table 5 - Genome statistics of of Citrobacter portucalensis strain Sb-2

Attribute	Value	% of Total
Genome size (bp)	4,794,853	100.00
DNA coding (bp)	4,279,139	89.2[a]
DNA G + C (bp)	2,491,072	51.9[a]
DNA Scaffolds	37	100.00
DNA contigs	40	
Total genes	4,551	100.00
Protein coding genes	4,430	97.3[b]
RNA genes	8 (rRNA) 73 (tRNA)	1.8[b]
Pseudo genes	32	0[b]

[a]Relative to genome size

[b]Relative to total number of genes

Table 6 - Prophages observed in Citrobacter portucalensis strain Sb-2 or P10159 (NZ_CP012554), Citrobacter freundii strain RHB12-C20 (NZ_CP057863) or R17 (NZ_CP035276) and Citrobacter braakii strain FDAARGOS_253 (NZ_CP020448)

Strain replicon	Region Length (Kb)	Completeness [a]	Score [b]	Total Proteins	Region Position		Most Common Phage [c]
Sb-2* NZ_JAEKIJ01000003	41.4	questionable	70	15	733,649	775,108	PHAGE_Escher_500465_1 (NC049342)
NZ_JAEKIJ01000004	34.4	intact	150	43	224,155	258,606	PHAGE_Salmon_SP_004 (NC_021774; 21)
NZ_JAEKIJ01000004 ***ars*$_2$ - cluster**	59.3	intact	150	67	493,978	553,282	PHAGE_Klebsi_phiKO2 (NC_005857; 14)
NZ_JAEKIJ01000006	6.6	incomplete	10	10	164,276	170,902	PHAGE_Pectob_CBB (NC_041878; 2)
NZ_JAEKIJ01000013 ***ars*$_1$ - cluster**	25.5	intact	150	35	14,000	39,213	PHAGE_Entero_mEp237_NC_019704(14)
P10159	19.2	incomplete	30	7	479,161	498,440	PHAGE_Escher_RCS47_NC_042128(4)
	20.4	incomplete	50	9	976,563	996,990	PHAGE_Salmon_SEN34_NC_028699(2)
	32.2	questionable	80	37	1003041	1035284	PHAGE_Pectob_ZF40_NC_019522(12)
	46.4	intact	150	69	1231786	1278264	PHAGE_Entero_HK225_NC_019717(9)
	11.8	questionable	75	13	2158000	2169802	PHAGE_Entero_P4_NC_001609(7)
	14.8	incomplete	30	18	2685034	2699901	PHAGE_Escher_phiV10_NC_007804(2)
	10.5	incomplete	30	12	2721342	2731893	PHAGE_Entero_P4_NC_001609(6)
	39.9	questionable	90	51	3488390	3528292	PHAGE_Cronob_ESSI_2_NC_047854(26)
	12.8	incomplete	10	16	3576586	3589441	PHAGE_Klebsi_ST13_OXA48phi12.1_NC_049453(5)
	25.6	incomplete	10	15	4085587	4111207	PHAGE_Klebsi_ST437_OXA245phi4.1_NC_049448(3)
	45.9	questionable	70	19	4127808	4173737	PHAGE_Escher_500465_1_NC_049342(12)
	44.1	intact	98	51	4278053	4322211	PHAGE_Escher_phiV10_NC_007804(35)
***ars*$_1$ - cluster**	27.2	incomplete	30	19	4842885	4870087	PHAGE_Entero_HK225_NC_019717(3)
	9	incomplete	60	14	4876401	4885459	PHAGE_Entero_mEp237_NC_019704(5)
	28.5	incomplete	60	16	4900611	4929135	PHAGE_Salmon_SEN34_NC_028699(11)
	14.1	incomplete	30	14	4934090	4948208	PHAGE_Salmon_118970_sal3_NC_031940(3)
	31.7	questionable	80	43	5026345	5058082	PHAGE_Entero_mEp237_NC_019704(16)
	15.8	intact	100	21	5056738	5072597	PHAGE_Salmon_118970_sal3_NC_031940(9)
RHB12-20	40.4	intact	94	54	706.748	747.237	PHAGE_Salmon_SEN8_NC_047753(31)
	49.9	questionable	70	15	1.262.439	1.312.361	PHAGE_Escher_500465_1 (NC_049342; 12)
	46	intact	110	58	1.418.724	1.464.723	PHAGE_Salmon_SPN1S (NC_016761;34)
	39.4	intact	150	56	1.595.200	1.634.667	PHAGE_Entero_SfV (NC_003444; 21)
	7.6	incomplete	20	8	1.647.496	1.655.131	PHAGE_Escher_500465_2 (NC_049343; 5)
***ars* - cluster**	29.1	incomplete	60	24	2.144.805	2.173.926	PHAGE_Entero_mEp237 (NC_019704; 5)
	26.1	incomplete	40	24	2.872.645	2.898.824	PHAGE_Erwini_vB_EhrS_59 (NC_048198; 4)
	48.9	intact	130	65	2.983.247	3.032.209	PHAGE_Entero_Sf101 (NC_027398;12)
	45.9	questionable	90	35	3.120.189	3.166.107	PHAGE_Entero_mEp237 (NC_019704;10)
	40.3	intact	150	46	3.394.290	3.434.683	PHAGE_Entero_phiP27 (NC_003356; 7)
	28.8	incomplete	30	7	4.668.521	4.697.357	PHAGE_Escher_RCS47 (NC_042128; 7)
R17	12,3	incomplete	20	16	111673	124005	PHAGE_Entero_phiP27_(NC_003356; 2)
	41.8	questionable	70	15	1292269	1334070	PHAGE_Escher_500465_1 (NC_049342; 12)
	48	intact	150	83	1609416	1657477	PHAGE_Edward_GF_2 (NC_026611; 24)
	48.1	intact	130	68	1791560	1839691	PHAGE_Salmon_118970_sal3 (NC_031940; 29)

	28	questionable	90	17	4620611	4648666	PHAGE_Stx2_c_1717 (NC_011357; 3)
	12,3	incomplete	20	16	111673	124005	PHAGE_Entero_phiP27 (NC_003356; 2)
253	59.3	intact	150	67	375860	435234	PHAGE_Klebsi_phiKO2_NC_005857; 14)
***ars* - cluster**	22	intact	140	22	1091018	1113061	PHAGE_Klebsi_phiKO2_NC_005857; 16)
	24,2	incomplete	40	25	1110719	1134990	PHAGE_Entero_mEp237_NC_019704; 9)
	49.1	intact	150	52	1297820	1346948	PHAGE_Phage_Gifsy_2_NC_010393; 20)
	33.8	intact	150	41	1708630	1742517	PHAGE_Salmon_Fels_2_NC_010463; 30)

(*) No complete sequence available for sorting to replicons. (a) Prediction of whether the region contains an intact or incomplete prophage,(b) score based on PHASTER criteria (Arndt et al. 2019; Zhou et al. 2011) (c) the phage with the highest number of proteins most similar to those in the region (between parentheses: accession number; number of proteins). Green rows show *arsH* <-> ***arsRBC*** clusters flanked by phages and yellow rows show ***arsRDABC*** <-> ***arsR*$_1$** <-> ***yraQ*** clusters enclosed by phages.

Figures

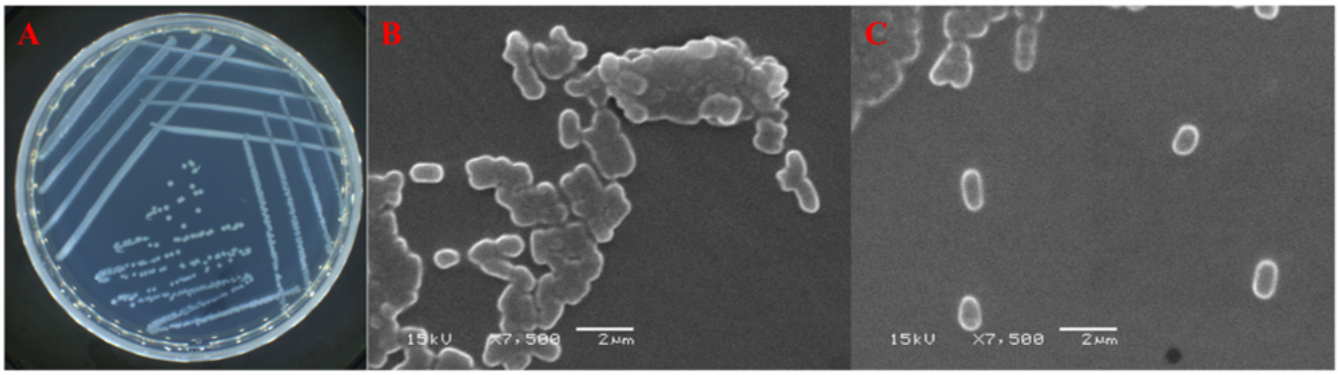

Figure 1

Colony morphology on minimal salts medium (A) and cell morphology (B, C) of Citrobacter sp. Sb-2 observed by SEM (scanning electron microscopy).

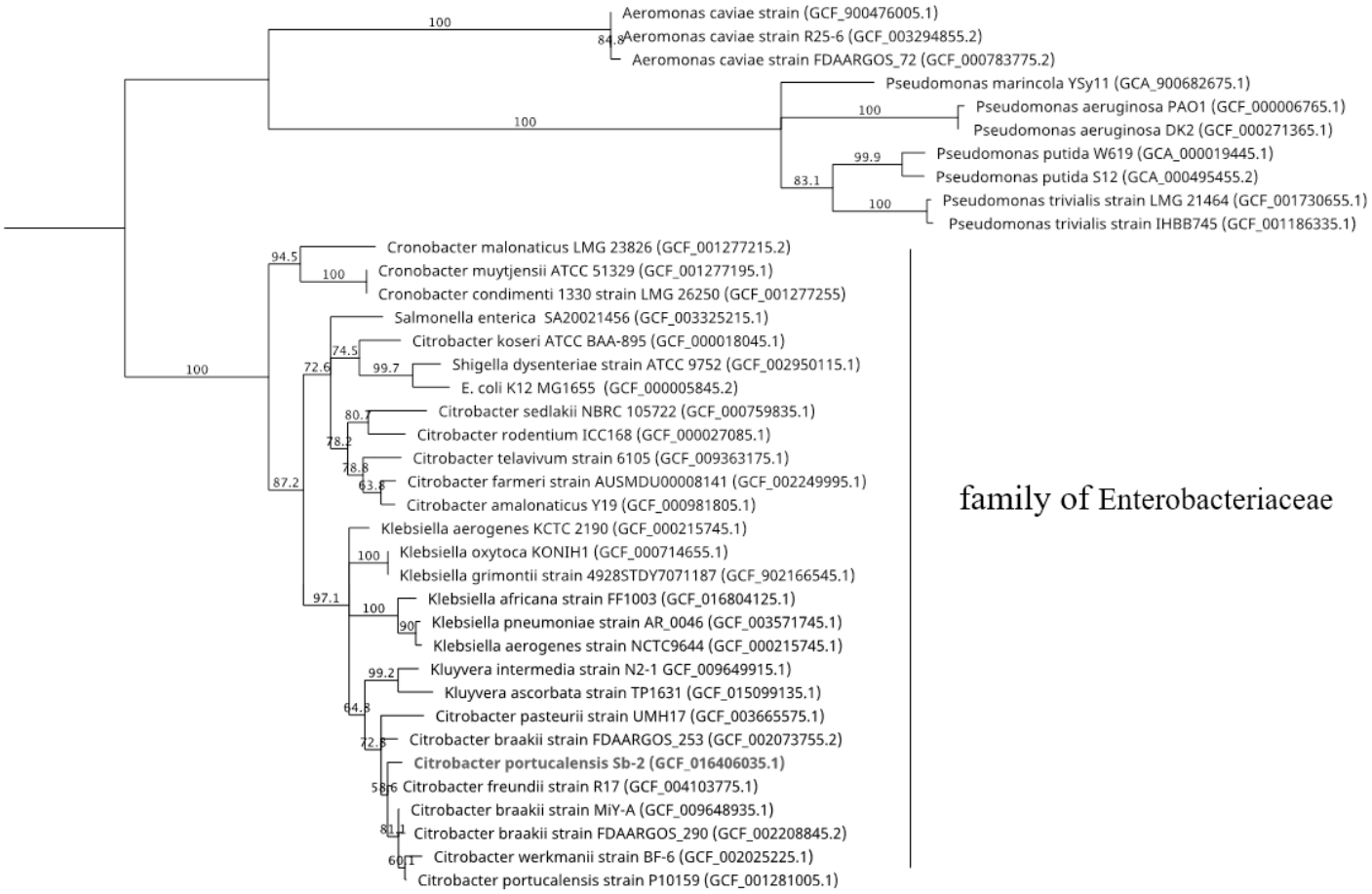

Figure 2

Molecular Phylogenetic tree based on the 16S rRNA gene (1,533 bp) sequences highlighting the position of Citrobacter portucalensis strain Sb-2 relative to other type and non-type strains of the genus Citrobacter (e.g. Enterobacteriaceae) and as outgroup the genus Aeromonas & Pseudomonas. RefSeq assembly accession numbers are shown in parenthesis. The evolutionary history was inferred by using the Geneious prime 2021.0.3. (Geneious Alignment Tree Builder) (https://www.geneious.com), global alignment with free gaps, identity (1.0/0.0), gap open penalty 12, gap extension penalty 3, 2 refinement iterations, Genetic Distance Model Jukes - Cantor, Neighbor - Joining, Resampling Method - Bootstrap. The tree was drawn to scale, with branch lengths calculated using the average pathway method; the scale bar corresponds to the number of substitutions per site, the branch labels are consensus Support (%) and Node Heights (Kearse et al., 2012).

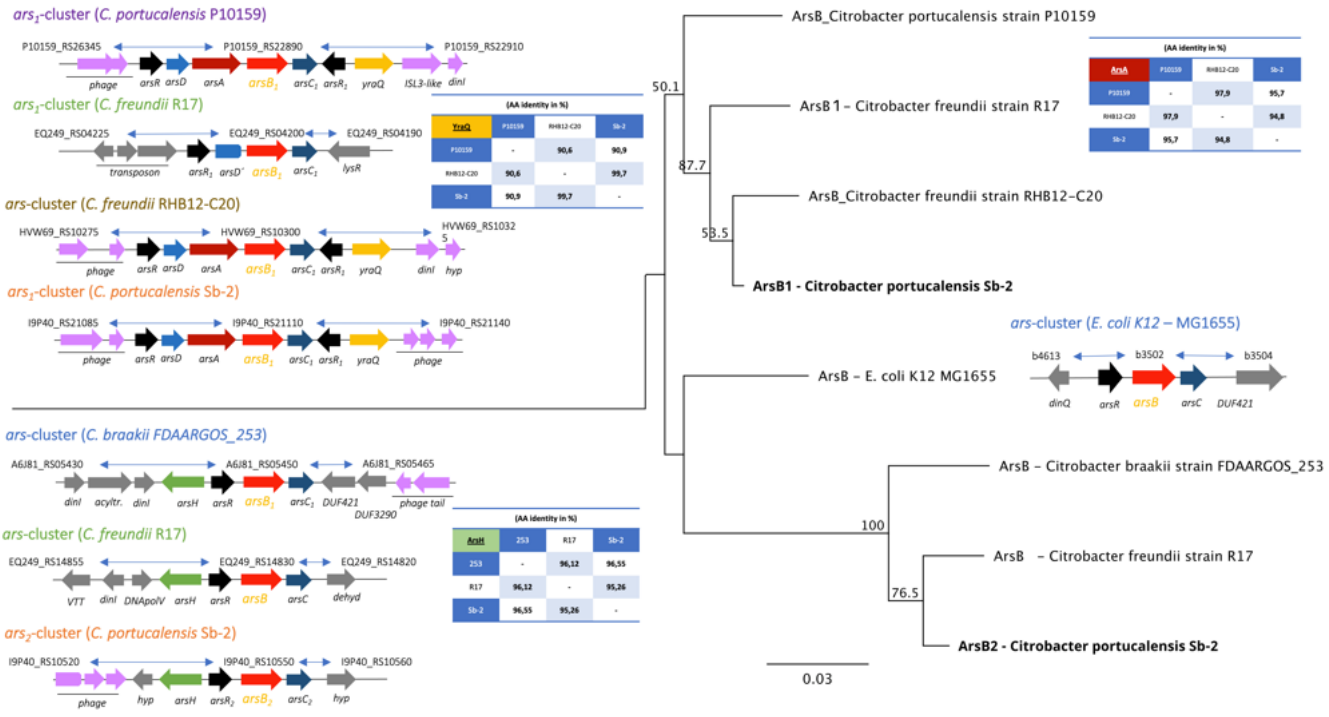

Figure 3

Comparison of the ars clusters - synteny and homology of the Citrobacter portucalensis Sb-2 & P10159, Citrobacter freundii R17 & RHB12-C20 and Citrobacter braakii FDAARGOS_253 to E. coli K12-W3110 as reference and Molecular Phylogenetic tree based on the full amino acid sequences of ArsB. In red genes encoding arsenical membrane transporter (ArsB), in dark red genes encoding arsenical pump-driving ATPases (ArsA), in blue genes encoding a metallochaperone protein (ArsD), in black genes encoding a arsenical resistance operon repressor (ArsR), in dark blue genes encoding arsenate reductase (ArsC), in yellow genes putative encoding a permease transporter (YraQ), in green genes encoding organoarsenical oxidase (ArsH), in violet phage-like genes, ~ predicted by PHASTER (Arndt et al. 2019) (hyp = hypothetical gene). For phylogenetic tree, the evolutionary history was inferred by using the Geneious prime 2021.0.3 (Geneious Tree Builder) (https://www.geneious.com), global alignment, gap open penalty 12, gap extension penalty 3, Blosum62 cost matrix, Jukes - Cantor, Neighbor - Joining). The tree was drawn to scale, with branch lengths calculated using the average pathway method; the scale bar corresponds to the number of substitutions per site (Kearse et al. 2012).

Supplementary Files

This is a list of supplementary files associated with this preprint. Click to download.

- Graphicalabstract.docx